



Strömgren photometry of ω Cen Red Giants.

A. Calamida¹, G. Bono^{2,3}, P.B. Stetson⁴, G. Iannicola³, A.M. Piersimoni⁵,
L.M. Freyhammer, R. Buonanno², F. Caputo³, S. Cassisi⁵, M. Castellani³, C. Corsi³,
M. Dall’Ora⁶, S. Degl’Innocenti⁷, I. Ferraro³, F. Grundahl⁸, M. Hilker¹, M. Monelli⁹,
M. Nonino¹⁰, A. Pietrinferni⁵, P.G. Prada Moroni⁷, L. Pulone³, and T. Richtler¹¹

¹ European Southern Observatory, Karl-Schwarzschild-Str. 2, D-85748 Garching bei München, Germany e-mail: acalamid@eso.org

² Università di Roma Tor Vergata, via della Ricerca Scientifica 1, 00133 Rome, Italy

³ INAF-OAR, via Frascati 33, 00040 Monte Porzio Catone, Italy

⁴ DAO, HIA-NRC, 5071 West Saanich Road, Victoria, BC V9E 2E7, Canada

⁵ INAF-OACT, via M. Maggini, 64100 Teramo, Italy

⁶ INAF-OAC, via Moiarriello 16, 80131 Napoli, Italy

⁷ Dipartimento di Fisica "E. Fermi", Univ. Pisa, Largo B. Pontecorvo 3, 56127 Pisa, Italy

⁸ Department of Physics and Astronomy, Aarhus University, Ny Munkegade, 8000 Aarhus C, Denmark

⁹ IAC, Calle Via Lactea, E38200 La Laguna, Tenerife, Spain

¹⁰ INAF-OAT, via G. B. Tiepolo 11, 40131 Trieste, Italy

¹¹ Universidad de Concepcion, Departamento de Fisica, Casilla 106-C, Concepcion, Chile

Abstract. We present new intermediate-band Strömgren photometry based on more than 300 u, v, b, y images of the Galactic globular cluster ω Cen, covering a region of more than 20×20 arcmin squared across the cluster center. By adopting different Strömgren metallicity indices we estimate the photometric metallicity for $\approx 4,000$ Red Giants, the largest sample ever collected. The metallicity distributions show multiple peaks ($[\text{Fe}/\text{H}]_{\text{phot}} = -1.69 \pm 0.08, -1.28 \pm 0.03, -1.07 \pm 0.02, -0.88 \pm 0.04, -0.71 \pm 0.12$ and -0.03 ± 0.08 dex) and a sharp cut-off in the metal-poor tail ($[\text{Fe}/\text{H}]_{\text{phot}} \lesssim -2$ dex) that agree quite well with spectroscopic measurements. We identify four distinct sub-populations, namely metal-poor (MP, $[\text{Fe}/\text{H}] \leq -1.49$), metal-intermediate (MI, $-1.49 < [\text{Fe}/\text{H}] \leq -0.93$), metal-rich (MR, $-0.95 < [\text{Fe}/\text{H}] \leq -0.15$) and solar metallicity (SM, $[\text{Fe}/\text{H}] \approx 0$). The last group includes only a small fraction of stars ($\sim 8 \pm 5\%$) and should be confirmed spectroscopically.

Key words. globular clusters: general — globular clusters: individual (Omega Centauri) — stars: abundances — stars: evolution

1. Introduction

The Galactic Globular Cluster (GGC) ω Cen, the most massive known in our Galaxy ($2.5 \times 10^6 M_{\odot}$, van de Ven et al. 2006), hosts

at least three separate stellar populations with a large undisputed spread in metallicity (Norris & Da Costa 1995, hereinafter ND95; Norris et al. 1996, hereinafter N96; Smith et al. 2000, Kayser et al. 2006, here-

inafter KA06). In particular, the recent high-resolution spectroscopic analysis of 180 Red-Giant (RG) stars by Johnson et al. (2008), hereinafter J08, provided a metallicity distribution with a dominant peak located at $[\text{Fe}/\text{H}] \approx -1.75$, and three secondary peaks at $[\text{Fe}/\text{H}] \approx -1.45$, -1.05 and -0.75 dex. This distribution agrees quite well with previous low- and medium-resolution spectroscopic metallicity distributions of main-sequence (MS) turn-off, sub-giant (SG) and RG stars (N96; KA06, Hilker et al. 2004), and the distributions obtained by Hilker & Richtler (2000), hereinafter HR00, ($\sim 1,500$ RGs) and by Hughes et al. (2004) (~ 2500 MS, SG, RG) using the Strömgren ($m_0, b-y$) metallicity diagnostic and by Sollima et al. (2005a) using the $(B-V)$ color of $\sim 1,400$ RG stars.

We present a photometric metallicity distribution of a sample of $\sim 4,000$ ω Cen RGs, based on the new calibrations of the Strömgren index m_1 provided by Calamida et al. (2007), hereinafter CA07.

2. Discussion and conclusions

A set of 110 $uvby$ Strömgren images centered on the cluster ω Cen were collected in 1999 with the 1.54m Danish Telescope (ESO, La Silla). This data set has been supplemented with 30 $uvby$ images of the SW quadrant of ω Cen collected in 1999 with the same Telescope. During these nights a set of 112 HD standard stars have been observed in the $uvby$ bands. HD stars have been selected from the catalogs of photometric standards by Schuster & Nissen (1988) and by Olsen (1993). Together with the quoted images we also adopted a set of 210 vby images collected with the same Telescope in two observing runs (1993 and 1995, see Hilker 2000).

The photometry was performed adopting DAOPHOT IV (Stetson 1994) and the final calibrated catalog includes $\sim 180,000$ stars. The accuracy of the absolute zero-point calibration is ~ 0.02 mag for the u, v -band data and ~ 0.015 mag for the b, y -band data. Fore more details on the observations and data reduction see Calamida et al. (2009), hereinafter CA09.

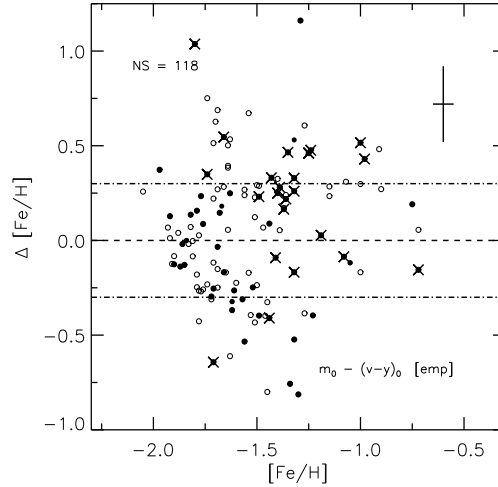


Fig. 1. Difference between photometric and spectroscopic metallicities, $\Delta[\text{Fe}/\text{H}] = [\text{Fe}/\text{H}]_{\text{phot}}(m_0, v-y_0)_{\text{emp}} - [\text{Fe}/\text{H}]_{\text{spec}}$, vs $[\text{Fe}/\text{H}]_{\text{spec}}$ for the 118 RG stars with accurate iron abundances by J08. Filled circles mark stars with the measurement of the spectroscopic S3839 index (VL07), while those for which this measurement is not available are marked with open circles. Crosses mark CN-strong stars according to both our selection (see CA09) and to ND95. The error bars account for both photometric and spectroscopic errors.

After cleaning the catalog for the contamination of field stars (see CA09), we selected only RGs with magnitudes $y \lesssim 16.5$ mag, $\sigma(u) \leq 0.02$ mag, $\sigma(v, b, y) \leq 0.015$ mag, and $\text{sep}(v, b, y) > 3$ (see Stetson et al. 2003), ending up with a sample of 3,953 stars.

To estimate the metal content of the selected ω Cen RGs we adopted the MIC relations provided by CA07 (see their Table 3) and based on the $u-y$ and on the $v-y$ color, together with the new MIC relation derived in CA09 and based on the $b-y$ color. The photometric metallicities were estimated using both the empirical and the semi-empirical calibrations. The individual metallicities were estimated by assuming for ω Cen a mean reddening value of $E(B-V) = 0.11$ and the extinction coefficients for the Strömgren colors discussed in Calamida et al. (2005).

To verify the accuracy of the metallicity estimates, we cross-correlated our RG sam-

ple with the iron abundances of the 180 RG stars provided by J08. We found 118 stars in common. Moreover, to constrain on a quantitative basis the impact of possible CN enhancements we supplemented the previous spectroscopic catalog with the large set of medium-resolution spectra collected by van Loon et al. (2007), hereinafter VL07. We found 373 RGs in common with our photometric catalog. Fig. 1 shows the difference between photometric and spectroscopic iron abundances for the 118 RGs in common with J08¹. Filled circles mark the stars for which the measurement of the $S3839$ index (cyanogen band) is available (VL07), while the open circles represent stars which lack of this measurement. The crosses mark the CN-strong stars according to either our selection ($\delta CN > 0.2$, see CA09) or to that of ND95. Data plotted in this figure show that CN-strong stars are, as expected, concentrated among the more metal-rich stars ($[Fe/H] \gtrsim -1.5$, Gratton, Sneden & Carretta 2004). The mean difference between photometric and spectroscopic abundances, using the six different MIC relations, is $\Delta[Fe/H] = 0.05 \pm 0.03$ and $\sigma = 0.37$ dex.

It is worth mentioning that 25 out of the 118 stars show discrepancies in iron abundance larger than 0.3 dex. The measurement of the CN index is available for thirteen of these stars and among them ten are CN-strong. If we move the limit down to 0.2 dex, the number of discrepant stars is 46, and the CN index is available for 20 of them. The fraction of CN-strong stars becomes of the order of 75%. On the other hand, 17 stars show under-abundant photometric metallicities by more than 0.3 dex; among them ten have measurements of the CN index and only two are CN-strong stars. The current findings thus indicate that stars with large *positive discrepancies* in the photometric metallicity are highly correlated with the occurrence of strong CN bands. The stars with large *negative discrepancies* require a more detailed spectroscopic investigation to constrain their abun-

¹ Note that with $[Fe/H]$, we mean a global metallicity, i.e., the sum of the elements beyond helium without explicit assumptions concerning their relative distribution.

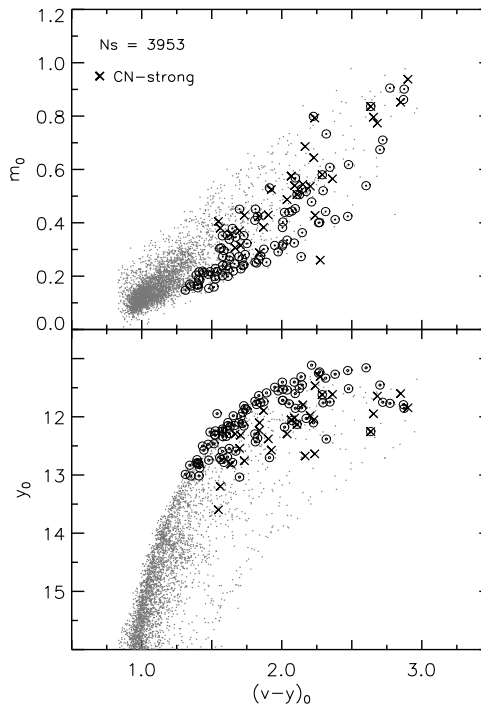


Fig. 2. Top: RGs of ω Cen in the $m_0, (v-y)_0$ plane. The open circles mark the 118 RGs from J08 and the CN-strong stars are marked with crosses. Bottom: Same as the top, but in the $y_0, (v-y)_0$ CMD.

dance pattern. If we neglect the CN-strong stars we find a mean difference of $\Delta[Fe/H] = 0.02 \pm 0.04$ and $\sigma = 0.37$ dex (93 stars).

As a final test of the intrinsic accuracy of the photometric abundances, we plotted the 118 RGs by J08 (open circles) onto the $m_0, (v-y)_0$ plane (Fig. 2, top panel) and in the $y_0, (v-y)_0$ plane (bottom panel).

It is noteworthy that stars for which the $S3839$ index measurement is available and are classified as CN-strong (crosses) according to our selection (CA09) or that of ND95 possess larger m_0 values and fainter apparent y_0 magnitudes at fixed color. This finding should not be affected by selection effects, since the low-resolution spectra collected by V07 cover a significant fraction of the RG branch in ω Cen (down to $V \sim 16$).

Fig. 3 shows the average metallicity distribution obtained adopting the $u-y, v-y, b-y$

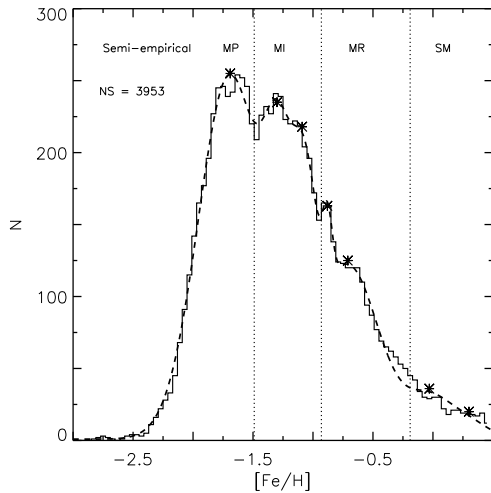


Fig. 3. Distribution of photometric iron abundances based on the semi-empirical calibrations of different MIC relations. The dashed line shows the fit of the metallicity distribution computed as the sum of seven Gaussians, and the asterisks mark the peaks. The vertical dotted lines display the different metallicity regimes: metal-poor (MP), metal-intermediate (MI), metal-rich (MR) and solar-metallicity (SM).

semi-empirical MIC relations. The individual distributions were smoothed with a Gaussian kernel having a standard deviation equal to the photometric error in the m_1 index. We fit the distribution with a sum of seven Gaussians and the dashed line plotted in Fig. 3 displays the cumulative fit, while the asterisks mark the position of the different Gaussian peaks: $[\text{Fe}/\text{H}]_{\text{phot}} = -1.69 \pm 0.08, -1.28 \pm 0.03, -1.07 \pm 0.02, -0.88 \pm 0.04, -0.71 \pm 0.12, -0.03 \pm 0.08,$ and 0.30 ± 0.08 dex. The large number of RGs allows us to identify four different metallicity regimes: metal-poor (MP) with $[\text{Fe}/\text{H}] \lesssim -1.5$ ($\sim 39 \pm 1\%$), metal-intermediate (MI) with $-1.5 \lesssim [\text{Fe}/\text{H}] \lesssim -1.0$ ($\sim 32 \pm 1\%$), metal-rich (MR) with $-1.0 \lesssim [\text{Fe}/\text{H}] \lesssim -0.2$ ($\sim 19 \pm 4\%$), and Solar metallicity (SM) with $[\text{Fe}/\text{H}] \approx 0$ dex ($\sim 8 \pm 5\%$, see vertical dotted lines in the figure). This last apparent sub-population lacks a firm spectroscopic confirmation. The limits of these metallicity regimes are arbitrary, though identified with the occurrence of either a local minimum or a shoulder in the metallicity distribution. The four main peaks

($-1.69 \leq [\text{Fe}/\text{H}] \leq -0.88$) agree quite well with low- (N96), medium- (Hilker et al. 2004; Sollima et al. 2005b) and high-resolution (J08) spectroscopic iron abundances and with previous photometric metallicities (HR00, S05a). Spectroscopic abundances also suggest the occurrence of metal-rich ($[\text{Fe}/\text{H}] = -0.60 \pm 0.15$) stars in ω Cen (ND95; Pancino et al. 2000). The stars belonging to the solar metallicity tail should be regarded with caution since they might be either CN-strong stars or field RGs.

References

- Calamida, A. et al. 2005, *AJ*, 634, L69
 Calamida, A. et al. 2007, *ApJ*, 670, 400 (CA07)
 Calamida, A. et al. 2009, *ApJ*, sub. (CA09)
 Gratton, R., Sneden, C., & Carretta, E. 2004, *ARA&A*, 42, 85
 Hilker, M. 2000, *A&A*, 355, 994
 Hilker, M., & Richtler, T. 2000, *A&A*, 362, 895
 Hilker, M., Kayser, A., Richtler, T., & Willemsen, P. 2004, *A&A*, 422, L9
 Hughes, J., Wallerstein, G., van Leeuwen, F., & Hilker, M. 2004, *AJ*, 127, 980
 Johnson, C.I., Pilachowski, C.A., Simmerer, J., Schwenk, D. 2008, *ApJ*, 681, 1505 (J08)
 Kayser, A., et al. 2006, *A&A*, 458, 777 (KA06)
 Norris, J.E., & Da Costa, G.S. 1995, *ApJ*, 447, 680 (ND95)
 Norris, J.E., Freeman, K.C., & Mighell, K.J. 1996, *ApJ*, 462, 241 (N96)
 Olsen, E.H. 1993, *A&AS*, 102, 89
 Pancino, E., et al. 2000, *ApJ*, 534, 83
 Schuster, W. J., Nissen, P. E. 1988, *A&AS*, 221, 65
 Smith, V. V., et al. 2000, *AJ*, 119, 1239
 Sollima, A., et al. 2005a, *MNRAS*, 357, 265 (S05a)
 Sollima, A., et al. 2005b, *AJ*, 634, 332
 Stetson, P. B. 1994, *PASP*, 106, 250
 Stetson, P. B., Bruntt, H., & Grundahl, F. 2003, *PASP*, 115, 413
 van de Ven, G., van den Bosch, R. C. E., Verolme, E. K., de Zeeuw, P. T. 2006, *A&A*, 445, 513
 van Loon, J.T., et al. 2007, *MNRAS*, 382, 1353 (VL07)